Earth Surface Processes and Landforms
Earth Surf. Process. Landforms, **23**, 1247–1267 (1998)

THREE-DIMENSIONAL MEASUREMENT OF RIVER CHANNEL FLOW PROCESSES USING ACOUSTIC DOPPLER VELOCIMETRY

S. N. LANE[1]*, P. M. BIRON[2], K. F. BRADBROOK[1], J. B. BUTLER[1], J. H. CHANDLER[3], M. D. CROWELL[1], S. J. MCLELLAND[4], K. S. RICHARDS[1] AND A.G. ROY[2]

[1]*Department of Geography, University of Cambridge, Downing Place, Cambridge, CB2 3EN, UK*
[2]*Département de Géographie, Université de Montréal, CP 6128, Succ. Centre-Ville, Montréal, Québec, Canada H3C 3J7*
[3]*Department of Civil Engineering, Loughborough University, Loughborough, LE11 3TU, UK*
[4]*Department of Geography, University of Exeter, Amory Building, Rennes Drive, Exeter, EX4 4RJ, UK*

Received 7 May 1997; Revised 18 May 1998; Accepted 22 May 1998

ABSTRACT

This paper describes and assesses: (i) the use of a new instrument for the determination of three-dimensional flow velocities in natural rivers, the acoustic Doppler velocimeter (ADV); and (ii) a method for positioning and orienting such measurements relative to a single local coordinate system to relate flow velocity vectors with the bed and water surface. The ADV uses the Doppler shift principle to measure the velocity of small particles, assumed to be moving at velocities similar to the fluid. Velocity is resolved into three orthogonal components, and measured in a volume 5 cm below the sensor head, minimizing interference of the flow field, and allowing measurements to be made close to the bed. A simple method for positioning and orienting the instrument using digital tacheometry is described, and is used to obtain velocity measurements concurrently with measurements of both bed and water surface topography. The paper includes a preliminary field assessment of the ADV by comparing velocity profiles with those generated from Marsh McBirney electromagnetic current meters, and a full field assessment of the position and orientation methodology. These results suggest that the recommended methods in combination with an ADV are able to provide reliable mean three-dimensional velocity field information and accurate bed and surface topography. © 1998 John Wiley & Sons, Ltd.

KEY WORDS: acoustic doppler velocimetry; rivers; flow velocity; water surface elevation

INTRODUCTION

Recent research has recognized the importance of flow structures in open channels (Ashworth *et al*., 1996), and the need to improve understanding of their generation and interaction with the channel bed. The need for these measurements to be made in three dimensions is illustrated by recent studies of river channel confluences. These have a complex flow structure which is thought to arise from three possible sources: (a) streamline curvature (e.g. Ashmore *et al*., 1992; Rhoads and Kenworthy, 1995, 1998); (b) flow separation over avalanche faces (e.g. Best and Roy, 1991; McLelland *et al*., 1996); and (c) turbulence generated due to shear between the convergent fluids (e.g. Biron *et al*., 1993). Current measurement methods in river channel confluences use two-dimensional electromagnetic current meters. Following from the important developments that these instruments allowed for river meanders (e.g. Hey and Thorne, 1975), a number of researchers have applied them to the measurement of confluence flow processes (e.g. Ashmore *et al*., 1992; Biron *et al*., 1993; McLelland *et al*., 1996; Rhoads and Kenworthy, 1995, 1998). The main problem that these instruments introduce is how to obtain three-dimensional data, when the most commonly used configuration of these instruments operates in only two dimensions. A number of solutions have been adopted. Rhoads and Kenworthy (1995, 1998) estimate qualitatively the magnitude of the mean velocity in the third component through combining conservation of mass with a high density of measurement and following analytical methods developed for river meanders (e.g.

* Correspondence to: Dr S. N. Lane, Department of Geography, University of Cambridge, Downing Place, Cambridge, CB2 3EN, UK
Contract/grant sponsor: NERC; contract/grant number: GR3/9715
Contract/grant sponsor: NSERC (Canada)
Contract/grant sponsor: The Royal Society
Contract/grant sponsor: Fitzwilliam College

CCC 0197-9337/98/131247–21 $17.50

Hey and Thorne, 1975). Alternatively, it is possible to measure two components of velocity twice, with the instrument being rotated through 90° between measurements, so providing three velocity components, with one component common to both measurement periods (e.g. McLelland *et al*., 1996; De Serres *et al*., in press). The two sets of measurements may then be normalized to the common velocity estimate. However, both methods take time, and if the flow structure is unsteady, due to morphological change or due to flow periodicities caused by instabilities in the flow structure (e.g. Biron *et al* ., 1993), then such methods may be inaccurate. This is compounded if strong flow acceleration and deceleration produced by rapid changes in bed topography invalidate the conservation of mass method. Indeed, Lane *et al*. (in review) show how unreliable this means of estimating the third component of velocity can be. As Rhoads and Kenworthy (1998) argue, description of flow structures in river channel confluences and explanation of their generating mechanisms require instantaneous three-dimensional measurements. Extension of field measurements to numerical modelling makes the information need even more important since three-dimensional models need three-dimensional data for verification purposes. Recent research has noted the need to investigate three-dimensional numerical models (Lane and Richards, 1998), if only to establish just how effectively depth-average models parameterize the effects of secondary circulation (Lane, 1998).

Despite this requirement, the need for field measurement of three-dimensional velocity information has yet to be matched by reliable field technology. This technology must do two things. First, it must provide an accurate estimate of the instantaneous, three-dimensional velocity at points of interest to the study. Second, and of equal importance, these three-dimensional velocities must be positioned and oriented correctly with respect to the boundary conditions (notably bed and water surface topography) that are responsible for those velocities. Without such positioning and orientation, the measures will have to be corrected after data collection, which may require assumptions to be made which are not supported by the field situation under investigation. In the case of numerical modelling this is even more important, as the velocity data required for verification purposes must be positioned and oriented within the same coordinate system as the topography being used to drive the flow model.

This paper is concerned with development of reliable field technology that addresses these two points. Recent technological developments have brought acoustic Doppler velocimetry to the stage in which the sensors are sufficiently robust for use in natural river channels, and able to provide instantaneous three-dimensional velocity information. Concurrently, developoments in field-based surveying, when harnessed to this type of instrument, may allow the flow information to be accurately positioned and oriented within a local coordinate system, whilst simultaneously yielding information on local bed topography and water surface elevation. With these issues in mind, the paper is divided into two sections. The first details the principles of operation of the acoustic Doppler velocimeter, and includes basic advice on some of the basic parameters that can control the quality of the results obtained, the need for careful data filtering before analysis, and a simple comparison with an electromagnetic current meter to allow potential users to gain some faith in the instrument's measurements. The second details a method for using this instrument within shallow streams, allowing simultaneous acquisition of bed topography, water surface and positioned and rotated velocity data in three dimensions. It includes an assessment of the quality of the results that this method can produce. Data are presented from two research projects, one focusing on confluences in an actively braiding gravel-bed proglacial stream in Switzerland and connected with verification of three-dimensional models of confluence flow processes, and the second concerned with a stable reach of upland gravel-bed stream in Scotland and connected with the development of improved means of parameterizing roughness effects in hydraulic models.

ACOUSTIC DOPPLER VELOCIMETRY: THEORY AND OPERATING PRINCIPLES

A current meter must meet certain practical and technical criteria (Kraus *et al*., 1994): (i) portability; (ii) mechanical and environmental ruggedness; (iii) minimal flow disturbance; (iv) minimal recalibration; (v) suitability for the specified purpose: and (vi) cost effectiveness. In recent years, the electromagnetic current meter has become popular for use in field environments given its portability, ruggedness and ability to provide instantaneous flow velocity information in two dimensions. However, it suffers from three problems: (i) a failure to measure the third dimension simultaneously; (ii) the potential problem of flow interference which

some studies suggest may be significant (e.g. Lane *et al*., 1993); and (iii) the problem of spatial averaging around the sensor head which limits the temporal resolution of the instrument (e.g. Soulsby, 1980; Roy *et al*., 1996a). The principle of acoustic Doppler velocimetry has been used for some time to monitor three-dimensional velocities in laboratory flumes and more recently to monitor three-dimensional flow processes in coastal zones (e.g. Thomson *et al*., 1989; Jones *et al*., 1994) and large rivers (e.g. Richardson *et al*., 1996). The field instruments involve incoherent acoustic Doppler techniques, which provide instantaneous velocity profiles in three dimensions, but which at present require a minimum flow depth of *c*. 5 m for operation. Recent developments in coherent acoustic Doppler processing techniques have resulted in an acoustic Doppler velocimeter (ADV) designed for single-point measurements in any field environment, which can overcome some of the problems associated with established current meters.

Basic principles

Acoustic Doppler velocimetry makes use of the Doppler frequency shift of emitted acoustic signals after reflection by small sound-scattering particles present in the flow, where the frequency shift is proportional to the particle velocity. As the speed of the wave is fixed, there will also be a shift in the wavelength of sound, which is inversely porportional to the scattering particles' velocity. The instrument reported herein is based upon wavelength rather than frequency shift, but with the wavelength shift expressed as a phase change. The changes in wavelength ($d\lambda$) and phase ($d\phi$) are related by:

$$\frac{d\lambda}{\lambda} = \frac{d\phi}{2\pi} \tag{1}$$

Applying Equation 1 to the Doppler relation produces:

$$U = \frac{c}{4\pi f}\frac{d\phi}{dt} \tag{2}$$

where c is the speed of sound in water; and f is the frequency at which the ADV is operating, which is 10 MHz in the ADV used in this study. In Equation 2 an additional factor of 2 appears as two Doppler shifts are involved, one seen by the particle and one by the receiver. The instrument samples as quickly as possible as this increases the precision of the estimate; the more times that the instrument can sample, the larger the number of samples used to determine the velocity estimate, and the more precise the estimate will be.

With estimation of the change in phase in a given time period from Equation 2, the speed of the scattering particles can be estimated which, assuming that the particles are small enough to be neutrally buoyant, can be assumed to be equal to the speed of the flow. The instrument estimates the change in phase using a method called pure coherent pulse-to-pulse processing (Zedel *et al*., 1996), where successive pairs of pulses are compared. This is done over a large number of pulses and the phase change is estimated from the covariance calculated from consecutive pairs of pulses:

$$\frac{d\phi}{dt} = \frac{1}{\tau}\operatorname{atan}\left(\frac{\sin\phi_t\cos\phi_{(t+\tau)} - \sin\phi_{(t+\tau)}\cos\phi_t}{\cos\phi_t\cos\phi_{(t+\tau)} + \sin\phi_{(t+\tau)}\sin\phi_t}\right) \tag{3}$$

where t = time; τ = time between pulse transmission; and the received signal is defined by $S_t = \cos\phi + i\sin\phi_t$ with $i = \sqrt{-1}$. As estimation of the phase shift is based upon correlations between pulse pairs; the strength of this correlation provides a useful index of quality control. A strong correlation implies that the phase shift is being estimated with some consistency, with the majority of the scattering particles being used to calculate the phase

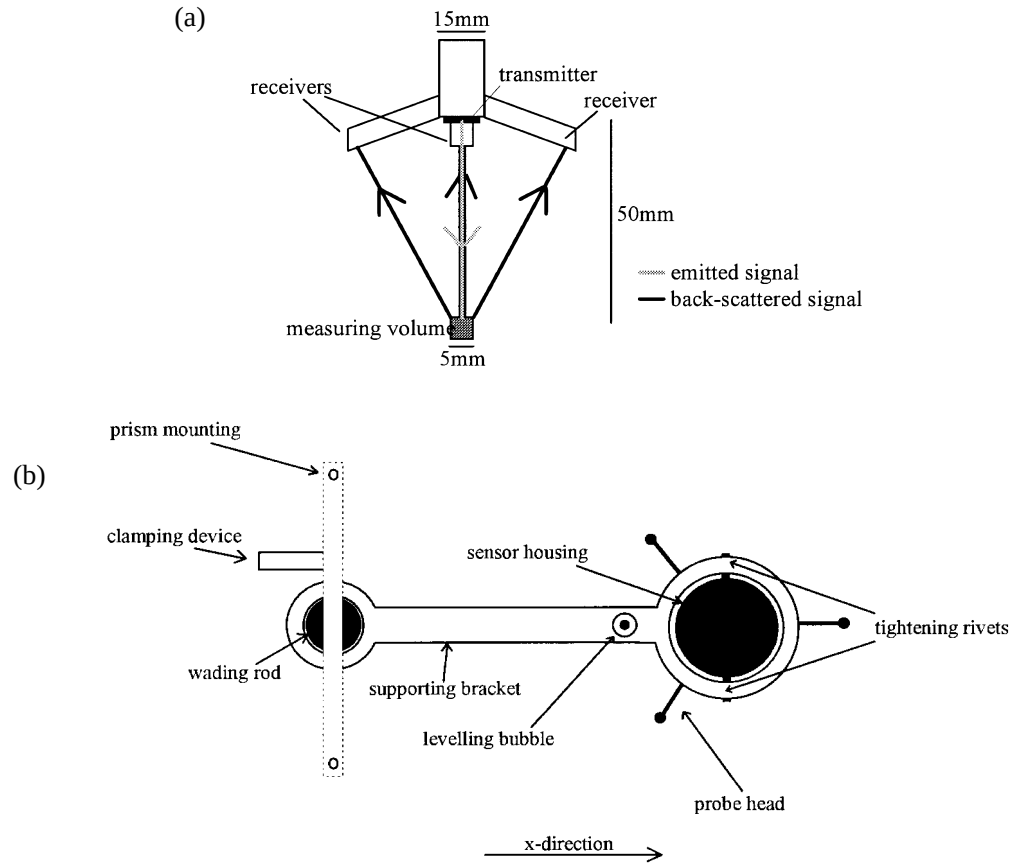

Figure 1. (a) View of sensor head and (b) planform view of wading rod (based upon Kraus *et al*., 1994). During setting up, it is necessary to ensure that the probe head is oriented such that the *x*-direction velocity as measured by the ADV is parallel to the supporting bracket, which sould be orthogonal to the prism mounting

shift moving in the same manner. The data are therefore likely to provide a reliable estimate of velocity. Random motions within the measuring volume and the advection of scatters through the measuring volume during the averaging process will decorrelate the signal, although the effect, which is essentially a loss of precision, may be reduced by increasing the frequency of pulse transmission (Zedel *et al*., 1996). This implies that close attention must be given to instantaneous signal correlations during measurement and low correlations will tend to be associated with highly turbulent flow, large velocity gradients within the sampling volume, the presence of large individual particles or interference from boundaries, all of which can reduce the coherence of the signal. Signal correlation is a key quality control parameter.

Three-dimensional measurements

The real advantage of the ADV is that through careful design of the probe head it is possible to measure all three dimensions of velocity instantaneously. Figure 1a shows the probe design of the ADV used in this study, manufactured by NorTek (see Further Information below). Three receiver transducers are mounted with 120° separation. They each receive sound scattered from a measuring volume, located 5 cm or 10 cm from the transmitter, depending upon instrument configuration. Given three receivers, and knowledge of their geometry, it is possible to resolve instantaneous velocities in three orthogonal directions. This probe also calculates the time taken for the transmitted sound to be reflected to the receivers from the bed, so allowing accurate determination of the elevation of the measuring volume above the bed. Although the instrument has yet to be

rigorously tested in field situations, calibration tests using a tow-carriage to measure velocities (Zedel *et al*., 1996) and laser Doppler velocimeter in both periodic flow conditions (Kraus *et al*., 1994) and uniform flow conditions (Voulgaris and Trowbridge, 1998) revealed very strong correlations between ADV velocities and independent measurements of flow velocity.

As with electromagnetic current meters, ADV operation requires careful consideration of a number of parameters during data collection, and notably specification of: (i) an expected velocity range; (ii) water temperature and salinity which together control the speed of sound in water; and (iii) the frequency with which data are recorded, which may be as high as 25 Hz. Each of these three issues needs careful consideration in any field campaign, particularly when taking measurements close to the boundary.

Expected velocty range and setting the maximum velocity

As the instrument operates upon detection of changes in phase, it is important that in a given τ, the change in phase is within the range $\pm\pi$, otherwise there is the possibility of aliasing. For instance, a phase change of $1{\cdot}5\pi$ has an identical effect upon Equation 3 as $-0{\cdot}5\pi$, even though the velocity associated with the former is much larger than the velocity associated with the latter. Thus, the maximum velocity that can be detected without aliasing has a phase change of $\pm\pi$. Applying this to Equation 2 produces the maximum detectable velocity:

$$U_{\max} = \frac{c}{4f\tau} \tag{4}$$

This would seem to suggest that for a given c and f, τ should be set as low as possible to allow the maximum detectable velocity to be as high as possible.

The total variance in a velocity signal will be the sum of the variance due to tubulent velocity fluctuations, the variance due to Doppler noise and the variance associated with the uncertainty in estimating the phase change. For turbulence studies, it is desirable that the velocity fluctuations are much greater than the instrument-generated error. For a given horizontal flow velocity and energy dissipation rate, the variance of the Doppler noise is inversely proportional to the velocity sampling time and the number of velocity measurements averaged in each sample (Voulgaris and Trowbridge, 1998). As a simple approximation, variance associated with the error of phase detection is proportional to τ^{-2} and the number of measurements averaged in each sample. Both of these suggest that τ should be as high as possible to minimize this effect. However, this will increase the possibility of aliasing. Thus, $U_{\max}$ should be set to as low a value as possible for the speed of the flow, as this will minimize the Doppler noise and phase detection error, without resulting in aliasing which could arise at lower values of $U_{\max}$. This issue is complicated by a link with the frequency with which data are recorded and these issues are considered in much more detail by McLelland and Nicholas (in prep.). $U_{\max}$ is set through the velocity range parameter: with a lower velocity range, τ is bigger, and hence the number of pulse pairs used to determine the phase change is smaller. Table I shows the velocity range settings used by the instrument, and the corresponding maximum horizontal and vertical velocities that can be measured with each of these settings. For instance, setting a velocity range of 10 cm s^{-1} means that the maximum horizontal velocity that can be detected is 60 cm s^{-1} and the maximum vertical velocity is 15 cm s^{-1}.

Speed of sound, temperature and salinity

It follows from Equation 2 above that the instrument is sensitive to the speed of sound in water, which is a function of both temperature (T) and salinity (s, measured in ppm). The sensitivities are given approximately by:

$$\frac{\mathrm{d}c}{\mathrm{d}T} = 0 \cdot 01, \frac{\mathrm{d}c}{\mathrm{d}s} = 0 \cdot 12 \tag{5}$$

Table I. The relationship between the ADV velocity range setting and the maximum horizontal and vertical velocities to avoid wrap-around. The elevation of the velocity hole, where the instrument is confused by the bottom-reflected signal, is also given for both the two standard probe configurations, one with the sampling volume 5 cm below the sensor head and the other 10 cm below the sensor head

ADV velocity range setting ($cm\,s^{-1}$)	Maximum horizontal velocity ($cm\,s^{-1}$)	Maximum vertical velocity ($cm\,s^{-1}$)	Elevation of velocity hole above boundary (5 cm probe) (cm)	Elevation of velocity hole above boundary (10 cm probe) (cm)
3	30	8	28	56
10	60	15	18	35
30	120	30	8	17
100	300	75	4	9

Thus, over long periods of measurement, it may be important to check environmental drift in either temperature or salinity and to correct the data collection process for this.

Frequency of data recording

In practice, there are two important frequencies that relate to the data recording process: (i) the internal frequency which ranges between *c*. 144 and *c*. 264 Hz; and (ii) the user-determined output frequency (25 Hz or less in the field instrument). The filter that acts between (i) and (ii) is essentially a block average, where the frequency and velocity range set by the user for data collection defines the number of time steps averaged: large numbers of measurements will be averaged at lower sampling frequencies and larger velocity ranges. For turbulence studies, it is important that the signal is filtered to remove Doppler noise, otherwise estimates of parameters such as turbulence intensity will be biased due to aliasing. As the nature of the Doppler noise is known (it is random, non-biased and Gaussian), it ought to be possible to filter the signal to remove it. However, this is complicated as under current arrangements, the field instrument block averages the signal to 25 Hz and research is needed to assess the extent to which this remains a problem. The laboratory instrument, which may be modified for field use (e.g. McLelland and Nicholas, in prep.), provides data at 100 Hz and so avoids this problem.

The sampling volume, spatial averaging and measurement close to boundaries

The size of the measuring volume is defined by the dimensions of the transmit and receive elements, the transmit pulse length and the timing of the receive window: when the receiver starts and stops listening determines which sound the instrument listens to, and hence where the sound is reflected from. The length of the transmit pulse is 4·8 μs, which, taken in combination with the speed of sound in water, produces a vertical pulse size of approximately 7·2 mm. The vertical extent of the sampling volume is determined by the timing of the receiving window and the beam pattern of the receive and transmit pulses to produce a typical vertical scale of 9 mm (Voulgaris and Trowbridge, 1998). The sampling volume width is approximately equal to the transmit ceramic width which is 7 mm. As the instrument averages over a number of pulses, the elevation of the sampling volume moves down during measurement by a small distance, which is about 0·15 mm. The greater the velocity range, the larger the number of pulses used, and hence the greater the displacement. As this displacement is so small, it is unlikely to distort velocity estimates significantly, except when the instrument is being used too close to a boundary, and one or more of the measurements is made where the sampling volume includes part of the boundary. This will result in at least one of the samples recording a phase shift of zero, which will both reduce correlation and produce a biased estimate of velocity, smaller than it really is. In practice, conditions will be rarely ideal when the boundary is rough, which may result in signal decorrelation with measurements where the sample volume is clearly above the boundary. This is because sound may be reflected from a number of points close to the measuring volume, so confusing the instrument.

The second problem with boundary measurement arises due to boundary interference. This occurs when the return signal from the boundary interferes directly with the return signal from the measuring volume, and may be particularly problematic with the downward-looking probe. It occurs when the time taken for one pulse to travel from the sampling volume to the boundary and back to the sampling volume is the same as the time

between pulses. It is therefore a function of τ and hence the velocity range set by the user. The effect is to produce a velocity 'hole' at certain elevations above the bed, where noise may mask the velocity signal. This is shown in Table I. Both of these problems need to be evaluated in terms of both sampling strategy in the field and the design of the specific probe being used. Figure 1a shows a downward-looking probe, which is ideally suited for boundary measurements in shallow streams. It is possible to use a sideward-looking probe, with a right-angle turn in the stem. The boundary problems described above are reduced for this probe design, and will be limited to measurements that are close to vertical channel walls, for instance. However, this design of probe is of less use when the real interest is in flow over rough beds, since a downward-looking probe is more effective for measuring flow around individual bed clasts.

In summary, this section emphasizes the following: (i) the need to give careful attention to the velocity range setting used during data collection; (ii) the importance of checking salinity and temperature changes, particularly if the instrument is deployed over long time periods to avoid drift; (iii) the need to treat measurements close to boundaries with some care; and (iv) the importance of the correlation parameter as the basic indicator of the quality of the velocity estimates being made.

ACOUSTIC DOPPLER VELOCIMETRY: DATA ANALYSIS

Preparatory data analysis

Following from the points made above, the ADV signals need to be inspected for poor signal correlation and, if the instrument is to be used for turbulence studies, the effects of aliasing. The signal correlation on each velocity component must be checked for each time step during measurement. With acoustic Doppler systems of the sort described here, a minimum acceptable correlation of 0·7 is recommended, and it is necessary to remove data points with correlations below this value. This can be undertaken using a freeware computer program (see Further Information section below) which processes batches of ADV-generated data files, allowing the user to remove instantaneous velocity values with low signal correlations, either using a general criterion that the average correlation should be greater than 0·7, or that every individual value should be greater than 0·7. Failure to remove velocity values with poor correlation will introduce bias into both mean velocity values and turbulence statistics. After removing velocity values, a new value is interpolated on the basis of the average of the immediately adjacent and acceptably measured nearest neighbours. This implies that both mean values and turbulence statistics will still contain bias, most notably reducing the variance of the signal and hence the magnitude of turbulence statistics (*cf*, Biron *et al*., 1995), although this will be less the case for mean values. The magnitude of the bias will be dependent upon the percentage of the series affected by poor correlations.

Figure 2 illustrates the importance of considering instrument correlations. In Figure 2a, the effect on mean velocity values is described, showing that where initial average correlations are less than 0·85, removal of poor correlations can result in a significant percentage change in the mean velocity values. Significant changes in average estimated velocity occur if less than 80 per cent of velocity values are retained after removing data points with low correlations (Figure 2b), and in isolated data series with percentages higher than this. The implications of such a removal and interpolating scheme for the derivation of turbulence statistics are serious. Even with 85 per cent of velocity values being retained, the amount of interpolation required will be sufficient to dampen variance and further investigation is required to assess the derivation of turbulence statistics using this instrument in field environments where instantaneous reductions in correlation (e.g. due to bed level change, small instruments movement or sediment transport) may be expected.

As the velocity time series measured by the ADV are affected by Doppler noise at frequencies greater than the Nyquist frequency (f_N) of the maximum sampling rate, aliasing will occur in the lower frequencies. The ADV allows field sampling at a maximum frequency (f_D) of 25 Hz, such that $f_N = 12{\cdot}5$ Hz. The noise must be removed from any series from which second or higher order moments are to be calculated. This may be achieved by low-pass filtering (O'Riordan *et al*., 1996) and in the research for this paper a filtering scheme was used that was developed and tested for laser Doppler anemometer data (Biron *et al*., 1995). This is based upon a Gaussian low-pass filter, which is simple, but allows both replicability and generality. The Gaussian smoothing function (wt) is defined as:

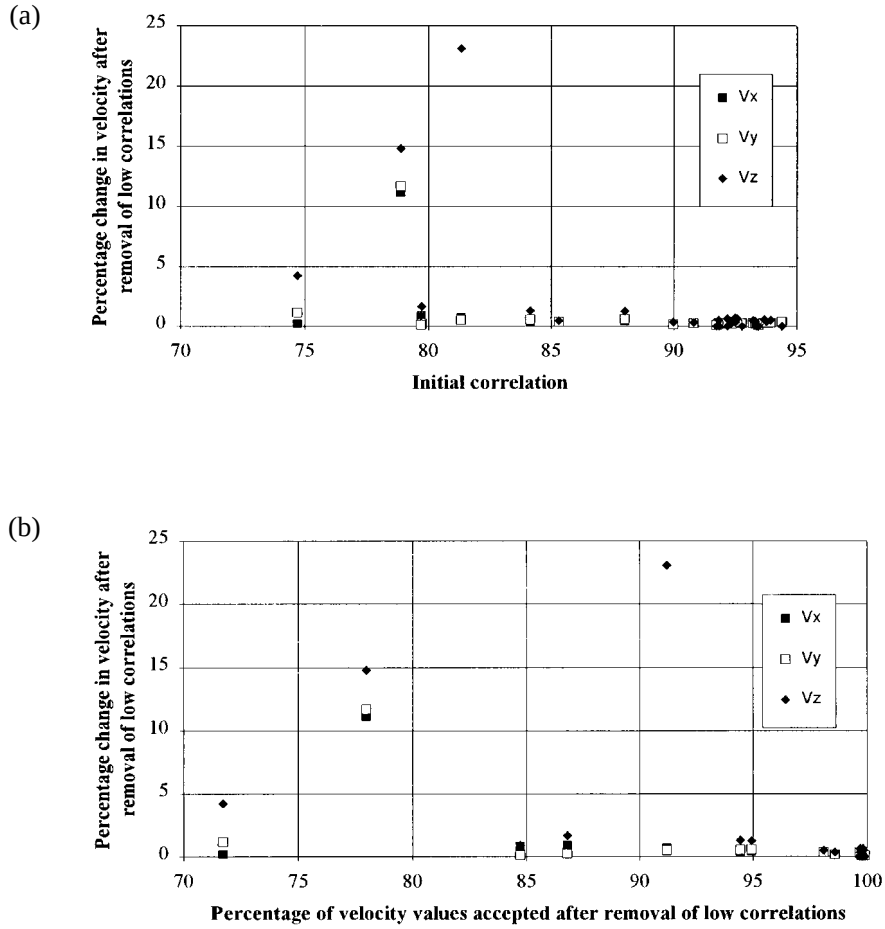

Figure 2. Plot of the percentage change in velocity after removing data with low correlation values versus (a) the initial correlation and (b) the percentage of velocity observations accepted after data removal. The change in velocity is calculated before interpolation of removed values

$$w(t) = (2\pi\sigma^2)^{-0.5} \exp(-t^2 / 2\sigma^2) \tag{6}$$

where

$$\sigma = \left(\frac{1n\,0 \cdot 5^{0.5}}{-2\pi^2 f_{50}{}^2} \right)^{0.5}$$

and $f_{50} = f_D/6$. This filter completely eliminates variance at frequencies greater than f_N, and severely reduces it at frequencies just below f_N, such that Doppler noise is completely eliminated. It also has the advantage of being very similar to the exponential filter used in Marsh McBirney electromagnetic current meters (ECMs) (Biron *et al.*, 1995; Roy *et al.*, 1997) and therefore facilitates comparisons between data collected with ADVs and ECMs.

Figure 3 shows how the low-pass filtering affects the power spectrum in the inertial range. The frequency spectra produced from unfiltered ADV velocity records characteristically flatten at high frequencies. Applying a Gaussian low-pass filter creates a sharp roll-off at high frequencies (Figure 3). The effects of the filter are also obvious in the time series, as it removes the high-frequency fluctuations (Figure 4), and in the root mean square

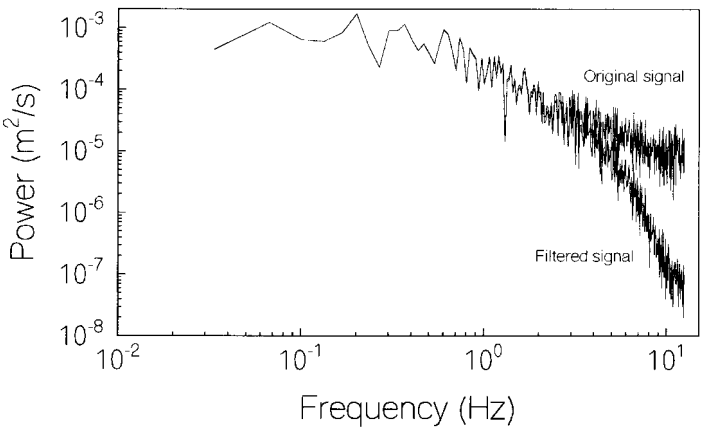

Figure 3. Power spectrum of a two minute streamwise-velocity signal collected at 25 Hz at 0·0179 m above the bed in a gravel-bed river before and after low-pass filtering with a Gaussian filter

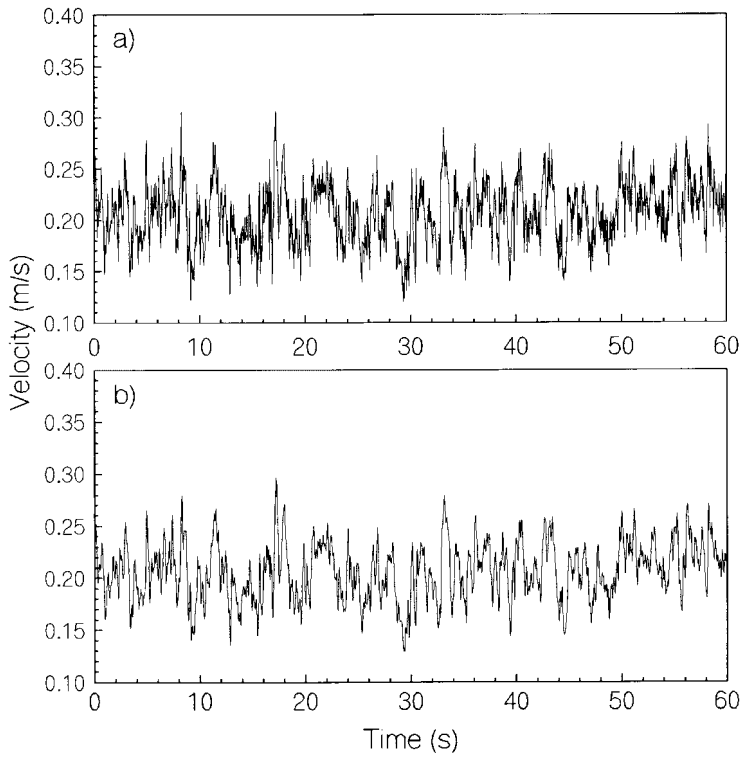

Figure 4. Time series of one minute of the signal presented in Figure 5: (a) prior to filtering (rms = 0·031 m s^{-1}); and (b) after filtering with a Gaussian filter (rms = 0·028 m s^{-1})

values which fall by about 10 per cent from 0·031 to 0·028. Unfortunately, given the current design of the field version of the instrument, there remains some uncertainty over the reliability of second-order estimates such as the root mean square of the velocity, if it is accepted that frequencies greater than 12·5 Hz are important. The user is only able to record the 25 Hz signal, which is already averaged over several pulses and is therefore already aliased. Dealing with this problem requires comparison with other instrumentation, further use of signal

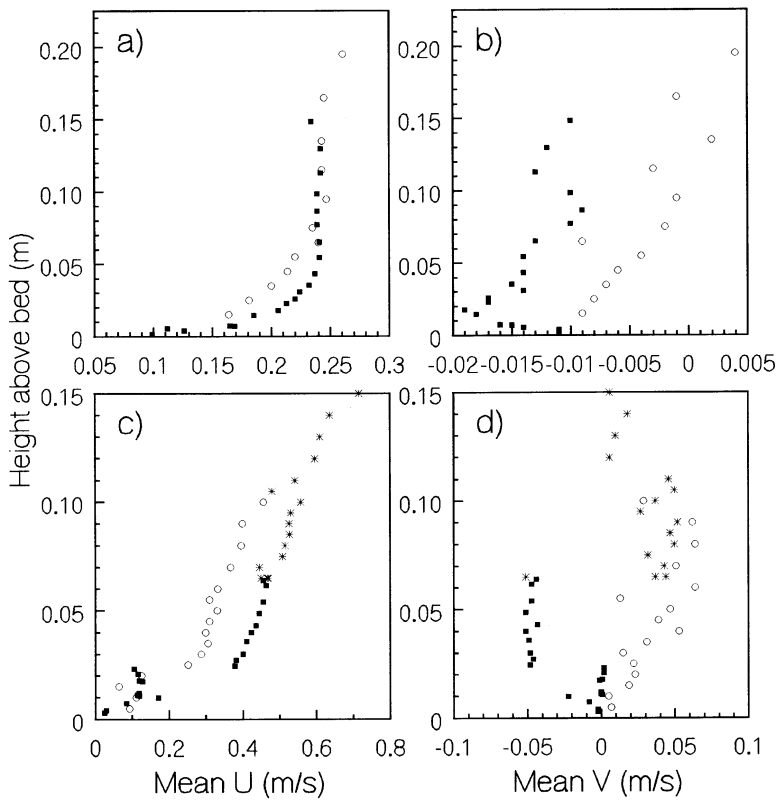

Figure 5. Velocity profiles collected from a clearwater gravel-bed stream on two separate occasions (a/b and c/d): (a) and (c) show mean downstream velocity values, and (b) and (d) show mean vertical velocity values. Symbol: ❍ = ADV; ■ = MMa; * = MMb

processing techniques, as well as careful reporting of the filter used so that comparisons of turbulence intensity data are meaningful (Roy *et al*., 1997). Voulgaris and Trowbridge (1998) undertook this assessment for an open-channel flume, with reassuring results. They found that the spectral estimates of the horizontal and vertical flow components agreed with theoretical spectral estimates after the latter were corrected for both problems of the Kolmogorov model (viscous dissipation and production effects) and the effects of the sensor (spatial averaging of the sampling volume and measurement noise variance).

Comparison with electromagnetic current meters for mean velocity estimates

One of the ways of establishing confidence in a measure of a process whose real nature is not known is through establishing coherence between two measures of the same phenomenon where the measuring instruments operate using two different physical principles (e.g. Hacking, 1983). Thus, comparison with an electromagnetic current meter has been undertaken for mean velocity, recognizing the difficulties of comparing higher moments of velocity estimates given instruments with different sampling volumes that use different filtering systems. This comparison was with two different Marsh McBirney electromagnetic current meters (MMa and MMb), each with a spherical sensor head of 0·013 m in diameter. On two separate occasions, each instrument was used to obtain a detailed vertical velocity profile at the same location in a clear-water stream in two different roughness environments: a sand-bed (D_{50} = 0·39 mm) and a gravel-bed (D_{50} = 21·4 mm) site (for further details, see Biron *et al*., 1998). Both instruments were oriented to measure the horizontal and vertical components of velocity without need for correction. Comparison of these measurements is shown in Figure 5, and the results are encouraging. For the horizontal velocity component, there was a good correspondence

between the ECM and the ADV over the sand-bed (Figure 5a), although some discrepancy is present at the bed. The ADV results may be more reliable as: (i) the instrument is able to measure with minimum flow field disruption; and (ii) it averages over a smaller measurement volume, which is likely to be significant close to the bed where velocity gradients are steepest and the averaging effect should be most apparent. Over the gravel bed, the correspondence between the ADV and MMa for the downstream component is strong near the bed but less good higher up in the flow (Figure 5c). However, the flow structure at this location was much more complex than for the sand bed location due to the significant effect of large protruding clasts which may generate eddy shedding. In this context, the agreement between both electromagnetic current meters and the ADV is reasonably good.

With respect to the vertical component, results are less reassuring. In Figure 5b, there is a clear but consistent discrepancy between estimates of vertical velocity: the shapes of the velocity profiles are similar, but there seems to be an instrument offset problem. There are two possible explanations: (i) that MMa had an offset problem in its vertical velocity component; or (ii) that both instruments were misaligned. Correct orientation is crucial for proper measurement of low-magnitude vertical velocity components, particularly when the downstream or crossstream velocities are of a high magnitude. In such cases, small rotation errors can result in the contamination of the vertical velocity with part of the higher downstream velocity component (Roy *et al*., 1996b). In Figure 5d, there is very little correspondence between the ADV and either MMa and MMb. This may be a product of the complex field environment in which this experiment was undertaken, with steep velocity gradients, where small differences in instrument position could produce large differences in recorded vertical velocity. Further correspondence checks, in the more controlled environment of the flume, are clearly required both to improve upon the assessment methodology reported here, and to extend it to turbulence statistics.

Conclusions

This section has described some of the basic principles of ADV operation, and the necessary post-processing, and has detailed a simple first attempt at instrument assessment. The latter suggests that the ADV is capable of reliable measurement of mean flow velocities, and further research (McLelland and Nicholas, in prep.) is exploring the use of ADVs for turbulence research. However, close attention must be given to: (i) parameters such as the velocity range setting used during data collection; (ii) the operation of the instrument close to boundaries, particularly with downward-looking probe design; and (iii) post-processing to remove poor correlations which will bias mean results and also filtering to remove aliasing.

FIELD POSITIONING AND ORIENTATION: METHODOLOGY AND ASSESSMENT

The second major aim of this paper was to describe a method for positioning and orienting the ADV in a local coordinate system, concurrent with measurement of both the river bed topography and water surface within the same system.

The field measurement system

A local site coordinate system is established using a digital tacheometer or total station and by constructing two survey stations adjacent to the area of interest. The required datum is defined by assigning arbitrary coordinates to one of the stations and assuming a bearing to the second station, to orient the spatial framework. The tacheometer can then be placed on either of the two stations, and oriented to the second. Subsequent measurement of the horizontal and vertical circles of the tacheometer and the slope distance to a survey prism enables the coordinates of any new point to be determined. To achieve this, the ADV may be mounted on a specially designed top-setting wading rod, which in our investigation was equipped with two survey prisms (Figure 1b) separated by 0·15 m. In use, the operator decides upon the planform position for a required velocity measurement and the rod is positioned so that the user and the rod are downstream of the ADV, and that the prisms are oriented towards the tacheometer, sufficient to get a return signal during electronic distance measurement. The use of two prisms means that the perpendicular to the prism axis does not need to point directly towards the tacheometer, so giving operators more flexibility in positioning the instrument and themselves. During measurement, the wading rod must be static, stable, aligned vertically and vibration free.

(a)

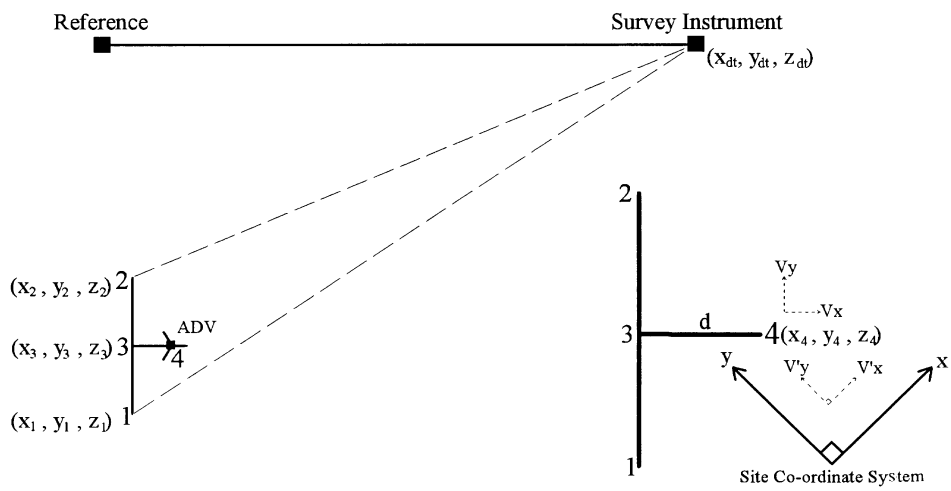

(b)

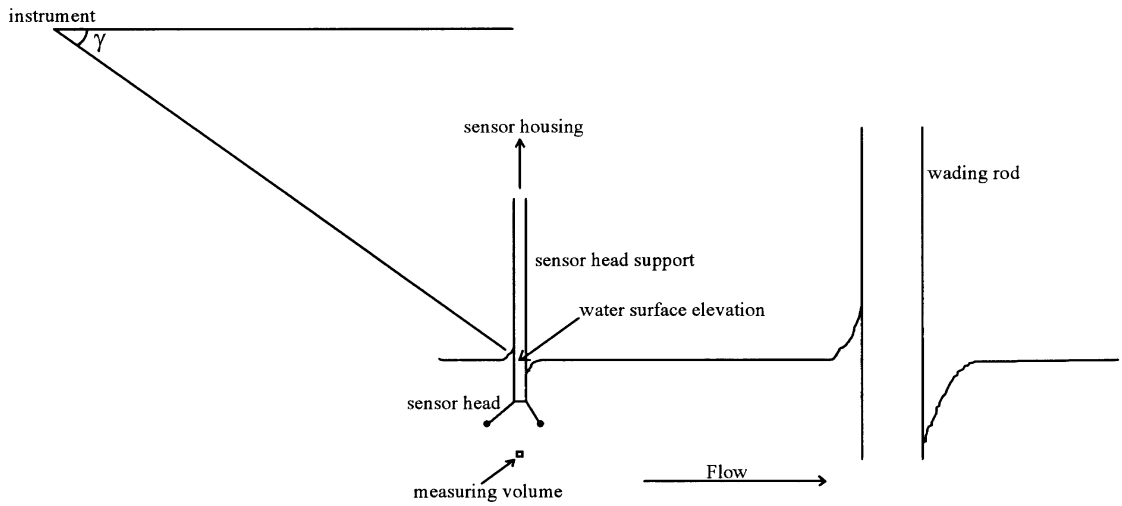

Figure 6. The nature of the rotation required to convert ADV velocities into those of a site coordinate system (a) and the measurement of water surface elevation (b) by measuring a vertical angle from the digital tacheometer to where the sensor head intersects with the water surface. Although the calculations were slightly more complicated than sighting to the wading rod, the smaller wake effect due to the thinner sensor head support provided more reliable results

This is facilitated by the handles, by a small plate on the base of the rod on which the rod operator may stand, and by a circular spirit bubble on the supporting bracket (Figure 1b). During the measurement process the tacheometer operator measures the horizontal and vertical circles and slope distance to both of the prisms, all data being recorded onto a data logger. An additional vertical circle reading is taken to the point where the ADV sensor head intersects the water surface, to allow estimation of the actual water surface at the sampling point. This is complicated by a wake effect (Figure 6b), considered below, whose magnitude is a function of both stream velocity and the diameter of the intersecting vertical rod. Sighting onto the wading rod makes the trigonometric calculations simpler, but its greater diameter results in a greater wake effect, so the sensor head support was used in these experiments.

These data are sufficient to determine the planform position of the ADV measuring volume and rotate the velocity information into the local coordinate system. To determine the elevation of the measuring volume, and subsequently the water surface elevation, it is only necessary to measure the vertical distance (D_v) of the measuring volume below the prism.

Calculation of the instrument position and subsequent velocity rotation

Determination of the ADV position, and orientation of the ADV sensor head into the local coordinate system, begins with determining the positions of the two prisms (1 and 2 in Figure 6a). From these, it is possible to determine the elevation of the measuring volume by substracting D_v from either prism elevation. The planform position of the ADV (or other current meter) at 4 is determined through calculation of the position of 3 in Figure 6a. The position 3 is:

$$x_3 = \frac{x_1 + x_2}{2}; y_3 = \frac{y_1 + y_2}{2} \tag{7}$$

where subscript indicates measurement position. The bearing of 3 to 4 is given by:

$$\beta_{34} = \beta_{12} + \frac{\pi}{2} = \text{atan}\left(\frac{x_2 - x_1}{y_2 - y_1}\right) + \frac{\pi}{2} \tag{8}$$

The standard *atan* function only returns an angle in the range –90° to +90° but it is advantageous and normal practice in UK surveying to convert this angle into an equivalent whole-circle bearing. This is achieved by examining the signs of the delta Eastings ($x_2 - x_1$) and Northings ($y_2 - y_1$), which determine in which of the four possible quadrants the flow direction lies, and adding π radians where necessary. The operation which carries this out is often known as the *atan 2* function and has two arguments, delta E ($x_2 - x_1$) delta N ($y_2 - y_1$).

As the distance, *d*, between 3 and 4 is known (the distance of the measuring volume from the wading rod), and because bearings are being used, the coordinates of 4 are given by quadrant-independent equations:

$$x_4 = y_3 + d \sin \beta_{34} \tag{9a}$$

$$x_4 = y_3 + d \cos \beta_{34} \tag{9b}$$

The survey data allow calculation of the prism elevation, and provided the wading rod was vertical during data collection, z_4 may be calculated by substracting the vertical distance between the measuring volume on the ADV and the prisms.

Again, because whole-circle bearings are being used, the rotated velocity components can be determined from quadrant-independent equations:

$$v'_x = v_x \sin \beta_{34} + v_y \cos \beta_{34} \tag{10a}$$

$$v'_y = v_x \cos \beta_{34} + v_y \sin \beta_{34} \tag{10b}$$

Equations 10a and 10b can be used to rotate mean or instantaneous values, but not standard errors. Rotated standard errors need to be determined by rotating the instantaneous values, and then calculating mean values. Given that the planform position of the measuring volume is (x_4, y_4), the water surface elevation (z_w) can be determined from:

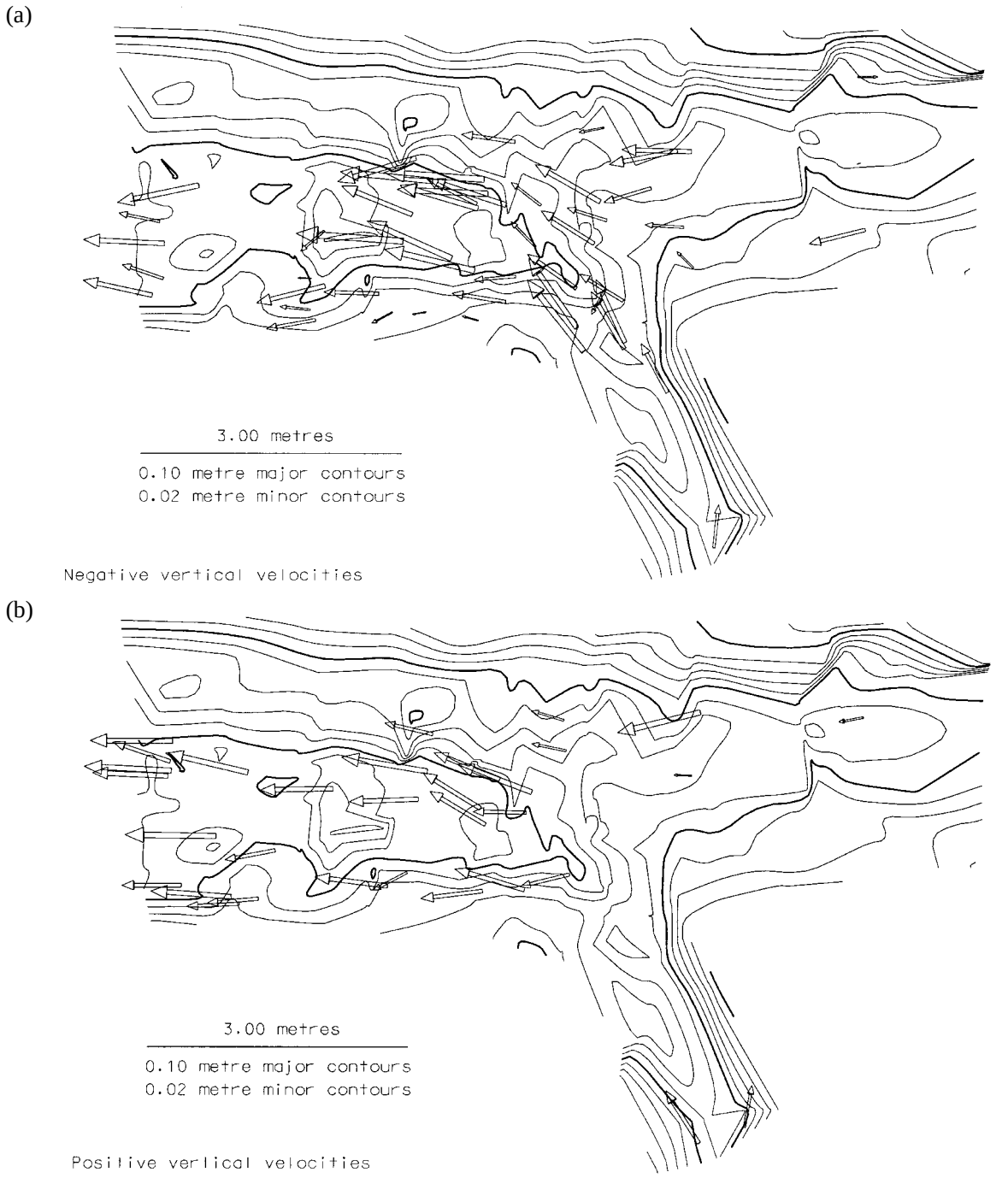

Figure 7. Plots of velocity vectors superimposed onto confluence morphology for 17 July dataset: (a) data with negative vertical velocities; (b) data with positive vertical velocities

$$z_w = z_{\mathrm{dt}} + h - \sqrt{(x_4 - x_{\mathrm{dt}})^2 + (y_4 - y_{\mathrm{dt}})^2}\,\tan\gamma \tag{11}$$

where z_{dt} is the height of the station at which the tacheometer is positioned; h is the height of the tacheometer above the station; (x_{dt}, y_{dt}) is the position of the tacheometer, and γ is the vertical angle between the horizontal and the bearing taken to the point of intersection of the sensor head support with the water surface.

As the ADV measures the elevation of the measuring volume above the stream bed (h_b), bed elevation can be determined from:

$$z_b = z_4 - h_b \tag{12}$$

Field results

Visualization of the results does allow a qualitative means of assessing the extent to which expected flow processes can be detected by the instrument. Figure 7 shows planform views of velocity vectors surveyed on the morning of 17 July 1995, between 8.30 and 11.30am before significant diurnal discharge increase, at a confluence fed by the Haut Glacier d'Arolla, Switzerland. Vectors with negative (Figure 7a) and positive (Figure 7b) vertical velocities are superimposed onto a bathymetric map with 5 cm contours. The confluence had a poorly developed scour-hole, and was dominated by large roughness elements. Nevertheless, there were strong negative vertical velocities into the confluence, particularly over the pronounced step leading from the true left tributary. Figure 7a also shows skewing of the tributary flow, some deflection of the main channel flow in response to the tributary discharge, with separation at the downstream junction corner, and then a progressive realignment of the general flow direction until it is parallel to the main channel direction. Positive vertical velocities occur downstream of the zone of strongly negative velocities, indicating the possibility of upwelling, as has been observed previously in some confluence configurations (Biron *et al*., 1993; De Serres *et al*., in press).

Assessment of the effectiveness of the planform rotation method

The research design described above aimed to determine the planform rotation parameter, and to minimize the effects of rotation in the other two axes around which it could occur through use of the spirit level that ensured that the instrument was vertical. This allows independent assessment of the effectiveness of this system because of the data redundancy involved. First, if the instrument is held vertical, the estimated heights of the two prisms should be idential. As this can be checked from the survey data, and as the prism spacing is known, the magnitude of tilt in the vertical plane parallel to the prism axis can be determined from:

$$\text{tilt} = \text{asin}\left(\frac{z_1 - z_2}{d_p}\right) \tag{13}$$

where d_p = prism separation distance measured on the wading rod. In practice, this tilt will be due to one of two effects: (i) error in the measurement of surveyed quantities; and (ii) actual tilt of the instrument; such that results from Equation 13 will be overestimates of tilt in this plane *per se*, although tilt in the plane orthogonal to the prism axis will introduce a second component of tilt.

Results from application to four test data sets (two from Arolla and two from Scotland) are shown in Figure 8 and Table II. These results are particularly encouraging with low mean values and a small standard deviation and range. It implies that tilt errors are generally less than ±3°. Tilt will have two effects: (i) it will cause components of the *x*- and *y*-direction velocities to be folded into the *z*-direction; and (ii) it will cause the measuring volume to be displaced by a distance (d_v on Figure 9) that reflects both the tilt error and the distance of the measuring volume above the bed, which will be particularly problematic where velocity gradients are steep. For the typical distances measured in the results reported in Figure 7, the measuring volume position displacement would be ±5–10 mm.

In addition to calculating tilt error, it is also possible to assess the planform rotation error. If the wading rod moves around its axis during measurement to each of the prisms (which takes 15 to 30 s), then this would be reflected in the surveyed distance between the prisms (d_o), which would be different from d_p, their separation

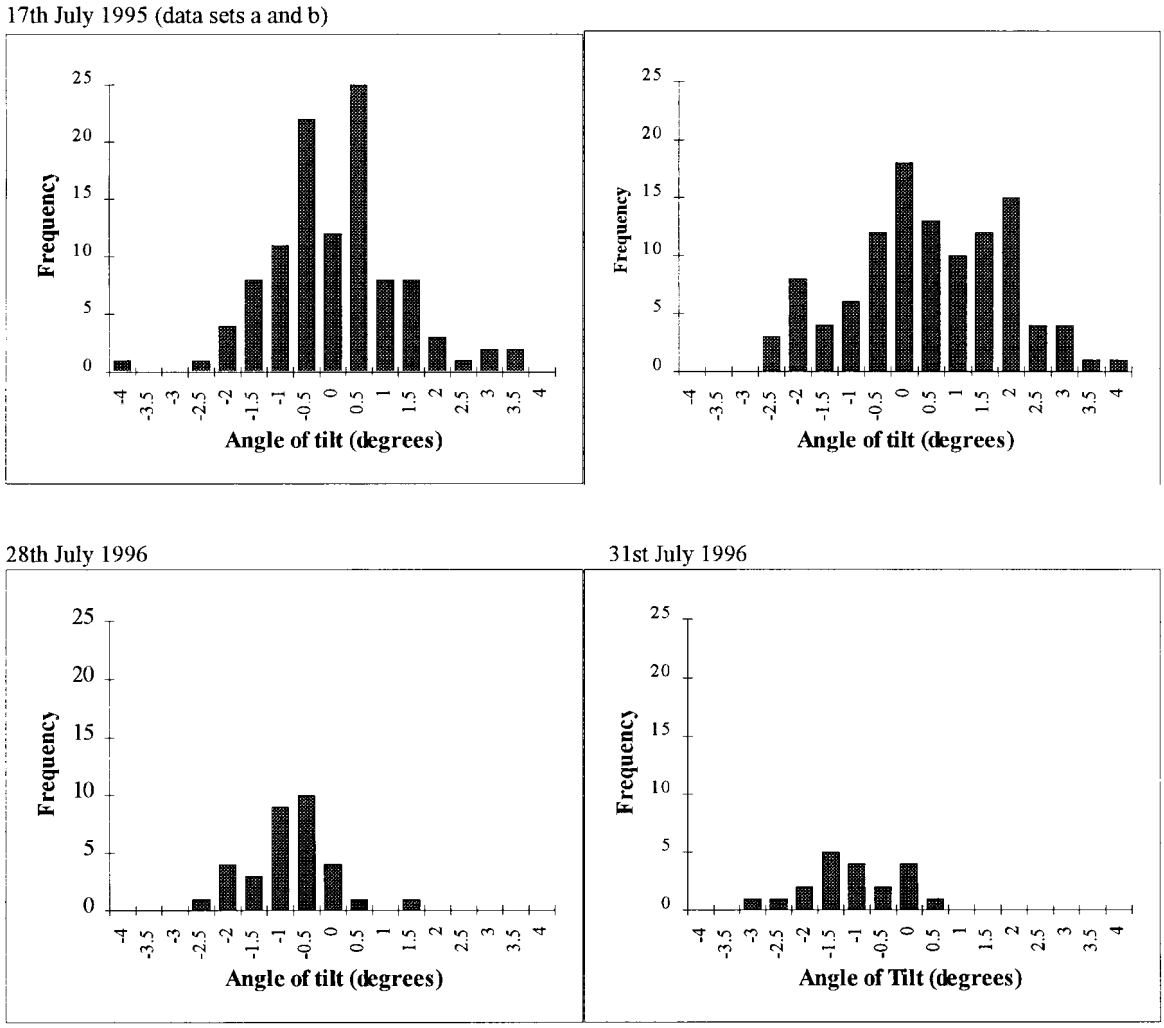

Figure 8. Four histograms of the tilt error calculated from the difference in elevations between the two surveying prisms

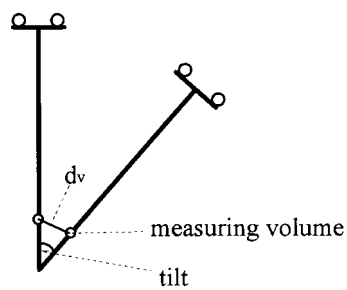

Figure 9. The effects of tilt error on the position of the measuring volume

Table II. Summary statistics for the tilt error calculated from the difference in elevations between the two surveying prisms (in degrees)

	17 July 1995 (a)	17 July 1995 (b)	28 July 1996	31 July 1996
Mean	0·288	0·708	–0·717	–0·842
Median	0·248	0·688	–0·611	–0·955
Standard deviation	1·230	1·450	1·147	0·857
Range	7·286	6·637	7·127	3·169
Minimum	–3·548	–2·405	–5·332	–2·519
Maximum	3·738	4·232	1·795	0·649
Count	108	111	34	20

distance (Figure 10). The magnitude of the error is an indication of the precision of estimation of flow direction. The rotation angle error (ρ) can be calculated from:

$$\frac{d_o}{d_p} = a\cos\left(\frac{\rho}{2}\right) \text{for } d_o < d_p \tag{14a}$$

$$\frac{d_p}{d_o} = a\cos\left(\frac{\rho}{2}\right) \text{for } d_o > d_p \tag{14b}$$

The results are shown in Figure 11 and Table III. They suggest that errors in flow direction may be as much as ±10°, although most observations are within ±5°, with a significant proportion within ±2° in all four cases. These are encouraging given previous research. Lane *et al.* (1995) have shown using ECMs that it is not possible to estimate planform rotation to better than ±20°. Planform error will cause uncertainty in the resolution of *x*- and *y*-direction velocities, and will also cause displacement of the measuring volume. With the wading rod used in this study, the measuring volume was always 0·3 m from the rod, and the displacement error (d_e) can therefore be calculated from:

$$d_e = \frac{0 \cdot 3\sin\rho}{\sin\left(\frac{\pi}{2} - \frac{\rho}{2}\right)} \tag{15}$$

With a rotation error of ±3°, this implies a displacement error of ±15 mm. This suggests that small rotation errors can significantly alter the expected position of the measuring volume, and this will need careful consideration when using these velocity estimates to assess numerical model performance. In particular, this error should be evaluated with respect to model grid size. Where the displacement error is greater than typical grid dimensions, ADV velocity estimates should be compared with velocities in the range of grid cells in which the measuring volume could have been positioned. Nevertheless, this error is comparable with the dimensions of the smallest ECM sensor heads, illustrating the precision that can be achieved using these methods.

In addition to providing indicators of the quality of the results that these methods can achieve, these assessments may be used to screen the acquired data. The following criteria were determined as acceptable for the data: (i) maximum acceptable tilt error of ±2°; (ii) maximum acceptable planform rotation error of ±5°; (iii) maximum measuring volume displacement due to both tilt and planform error of 5 mm. They may also be used to put error bands around individual velocity estimates when they are being used for other purposes (e.g. assessment of model performacne).

Quality of water surface elevation information

Unfortunately, there is no data redundancy that can be used to provide a check on the quality of the water surface information. The main uncertainty is the quality of the estimate of the vertical angle measured to the intersection between the sensor head support and the water surface, particularly in the presence of a wake effect. One way of obtaining an estimate of the precision of measurement of water surface elevation is by measuring

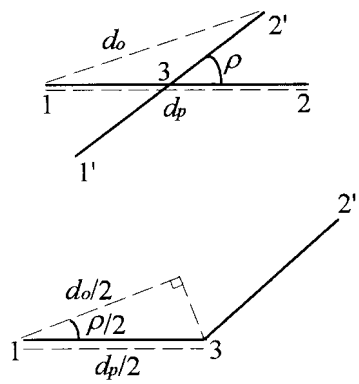

Figure 10. Calculation of the planform rotation error

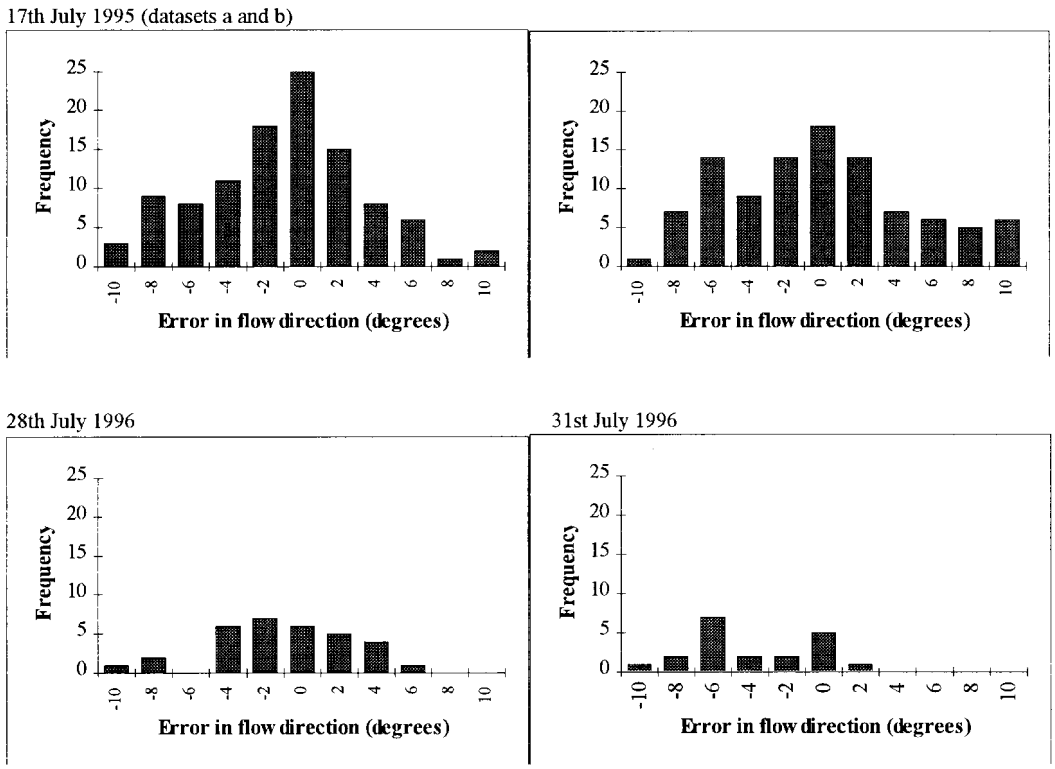

Figure 11. Four example histograms of the error in flow direction (ρ) calculated by comparing the known distance between prisms with that calculated from survey observations

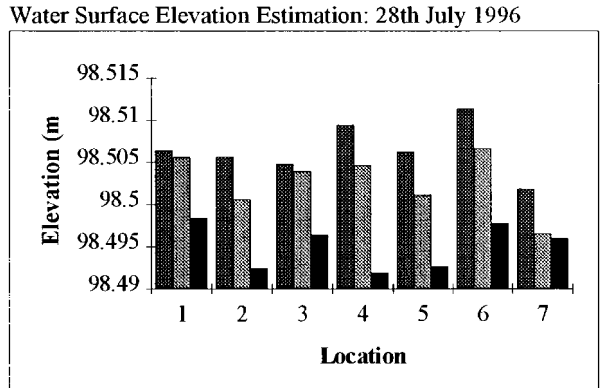

Figure 12. An illustration of the sensitivity of water surface elevation estimation. At each location, the first column refers to the estimated elevation of the wake top, the second column to the estimated elevation of the water surface and the third column to the estimated elevation of the wake bottom

Table III. Summary statistics for the error in flow direction calculated by comparing the known distance between prisms with that calculated from survey observations (in degrees)

	17 July 1995 (a)	17 July 1995 (b)	28 July 1996	31 July 1996
Mean	–0·077	–0·372	–1·071	–2·745
Median	0·334	0·0143	–0·584	–3·473
Standard deviation	4·455	7·751	5·140	3·417
Range	23·631	62·791	24·807	12·048
Minimum	–12·451	–21·461	–18·542	–9·094
Maximum	11·180	41·329	6·265	2·954
Count	108	111	34	20

vertical angles to both the wake top and the wake trough in addition to the sensor head support intersection. This was undertaken for a subset of points during one period of data collection, and Figure 12 shows the correponding elevation estimates. These results are encouraging, and suggest that it is possible to determine water surface elevations with a precision of at least ±5mm. The precision of the estimates will not be independent of survey design, as the effect of error in the estimation of vertical angles will be greater as the distance between the digital tacheometer and the wading rod increases. Furthermore, the size of the wake will change with the flow velocity and the precision will decrease.

CONCLUSION

This paper has described an integrated monitoring of river bed and water surface topography, and three-dimensional velocity data for river channel research. Although further field testing of the acoustic Doppler velocimeter is required, and particularly of its use in turbulence studies, it provides a robust and portable instrument that has much potential for small-scale, intensive investigation of interactions between river channel form and flow processes. There are two particular measurement advantages: (i) it measures all three dimensions of velocity simultaneously; and (ii) the measuring volume is remote from the sensor head. Appropriate research design allows the accurate and concurrent determination of other properties, such as bed elevation and water surface elevation, and the location and orientation of velocity measurements can be fixed into the same coordinate system as the topographic information. Detailed assessment of the quality of the acquired information is provided by the existence of data redundancy, and this can be used to minimize tilt and planform rotation errors by data screening. Current research is using datasets acquired from this integrated method to investigate the relationship between confluence morphology and flow patterns, to explore the interactions that

exist between bed roughness elements and flow structure, and to asses the output from three-dimensional numerical models applied to both situations.

ACKNOWLEDGEMENTS

This research is supported by NERC grant GR3/9715, NSERC (Canada), the Royal Society, Fitzwilliam College and research studentships awarded to K.F.B. and J.B.B. by NERC, and to M.D.C. by the Commonwealth Trust for Canada.

FURTHER INFORMATION

Further information on the SONTEK/NORTEK acoustic Doppler velocimeter may be obtained from: (i) HR Wallingford Ltd, for the UK (Ian Shepherd, Howberry Park, Wallingford, Oxon, OX10 8BA, Tel. 01491 835381, Fax. 01491 826344, Email: equipsales@hrwallingford.co.uk); (ii) NorTek, for the rest of Europe (NorTek, Bruksveien 17, N-1390 Vollen, Norway, Tel. +47-66-79-01-90, Fax. +47-66-79-04-20, Email: inquiry@nortek.com); and (iii) SonTek for elsewhere (SonTek, Inc., 7966 Arjons Drive, Suite D, San Diego CA 92126, USA, Tel. +619-695-8327, Fax. +619-695-8131, Email: inquiry@sontek,com).

The low-correlation data removing system was provided as freeware, through HR Wallingford, written by Tony L Wahl (Water Resources Research Laboratory, Technical Service Center, D-8560, US Bureau of Reclamation, PO Box 25007, Denver, CO 80225-0007, USA, Tel. +303-236-2000, ext. 446, Fax. +303-236-4096, Email: twahl@do.usbr.gov, WEB site: http://ogee.do.usbr.gov/twahl/winadv.html).

REFERENCES

Ashmore, P. E., Ferguson, R. I., Prestegaard, K. L., Ashworth, P. J. and Paola, C. 1992. 'Secondary flow in anabranch confluences of a braided gravel-bed stream', *Earth Surface Processes and Landforms*, **17**, 299–311.

Ashworth, P. J., Bennett, S. J., Best, J. L. and McLelland, S. J. (Eds) 1996. *Coherent Flow Structures in Open Channels*, Wiley, Chichester, 733 pp.

Best, J. L. and Roy, A. G. 1991. 'Mixing-layer distortion at the confluence of channels of different depths', *Nature*, **350**, 411–413.

Biron, P., De Serres, B., Roy, A. G. and Best, J. L. 1993. 'Shear layer turbulence at an unequal depth confluence', in Clifford, N. J., French, J. R. and Hardisty, J. (Eds), *Turbulence: Perspectives on Flow and Sediment Transport*, Wiley, Chichester, 197–214.

Biron, P., Roy, A. G. and Best, J. L. 1995. 'A scheme for resampling, filtering, and subsampling unevenly spaced laser Doppler anemometer data', *Mathematical Geology*, **27**, 731–748.

Biron, P. M., Lane, S. N., Roy, A. G., Bradbrook, K. F. and Richard, K. S. 1998. 'Sensitivity of bed shear stress estimated from vertical velocity profiles: the problem of sampling resolution', *Earth Surface Processes and Landforms*, **23**, 133–140.

Clifford, N. J. and Richards, K. S. 1992. 'The reversal hypothesis and the maintenance of riffle–pool sequences', in Carling, P. A. and Petts, G. E. (Eds), *Lowland Floodplain Rivers*, 43–70.

De Serres, B., Roy, A. G., Biron, P. M. and Best, J. L. (in press). 'Three-dimensional structure of flow at a confluence of river channels with discordant beds', *Geomorphology*.

Hey, R. D. and Thorne, C. R. 1975. 'Secondary flows in river channels', *Area*, **7**, 191–195.

Jones, S., Jago, C. F., Prandle, D. and Flatt, D. 1994. 'Suspended sediment dynamics: Measurement and modelling in the Dover Strait', in Beven, K. J., Chatwin, P. C. and Millbank, J. H. (Eds), *Mixing and Transport in the Environment*, 183–202.

Kraus, N. C., Lohrmann, A. and Cabrera, R. 1994. 'New acoustic meter for measuring 3D laboratory flows', *ASCE Journal of Hydraulic Engineering*, **120**, 406–412.

Lane, S. N. 1998. 'Hydraulic modelling in hydrology and geomorphology. A review of high resolution approaches', *Hydrological Processes*, **11**, 1131–1150.

Lane, S. N. and Richards, K. S. 1998. 'Two-dimensional modelling of flow processes in a multi-thread channel', *Hydrological Processes*, **11**, 1279–1298.

Lane, S. N., Richards, K. S. and Warburton, J. 1993. 'Comparison of high frequency velocity records obtained with spherical and discoidal electromagnetic current meters', in Clifford, N. J., French, J. R. and Hardisty, J. (Eds), *Turbulence: Perspectives on Flow and Sediment Transport*, Wiley, Chichester, 121–164.

Lane, S. N., Richards, K. S. and Chandler, J. H. 1995. 'Within reach spatial patterns of process and channel adjustment', in Hickin, E. J. (Ed.), *River Geomorphology*, 105–130.

Lane, S. N., Bradbrook, K. F., Richards, K. S., Biron, P. M. and Roy, A. G. (in review). 'Secondary circulation in river channel confluences: Measurement myth or coherent flow structure?', *Hydrological Processes*.

McLelland, S. J. and Nicholas, A. P. (in prep.).

McLelland, S. J., Ashworth, P. J. and Best, J. L. 1996. 'The origin and downstream development of coherent flow structures at channel junctions', in Ashworth, P. J., Bennett, S. J., Best, J. L. and McLelland, S. J. (Eds), *Coherent Flow Structures in Open Channels*, Wiley, Chichester, 459–490.

O'Riordan, C., Maldiney, M. -A., Mouchel, J. M. and Poulin, M. 1996. 'Un nouveau dispositif d'analyse du transport des matières en suspension dans les riviès', *Comptes rendus de l'Acadèmie des Sciences de Paris*, **322**, 285–292.

Rhoads, B. L. and Kenworthy, S. T. 1995. 'Flow structure in an asymmetrical stream confluence', *Geomorphology*, **11**, 273–293.

Rhoads, B. L. and Kenworthy, S. T. 1998. 'Time-averaged flow structure in the central region of a stream channel confluence', *Earth Surface Processes and Landforms*, **23**, 171–191.
Richardson, W. R. R., Thorne, C. R. and Mahmood, S. 1996. 'Secondary flow and channel changes around a bar in the Brahmaputra River, Bangladesh', in Ashworth, P. J., Bennett, S. J., Best, J. L. and McLelland, S. J. (Eds), *Coherent Flow Structures in Open Channels*, Wiley, Chichester, 519–544.
Roy, A. G., Buffin-Bélanger, T. and Deland, S. 1996a. 'Scales of turbulent coherent flow structures in a gravel-bed river', in Ashworth, P. J., Bennett, S. J., Best, J. L. and McLelland, S. J. (Eds), *Coherent Flow Structures in Open Channels*, Wiley, Chichester, 147–164.
Roy, A. G., Biron, P. and De Serres, B. 1996b. 'On the necessity of applying a rotation to instantaneous velocity measurements in river flows', *Earth Surface Processes and Landforms*, **21**, 817–827.
Roy, A. G., Biron, P. M. and Lapointe, M. F. 1997. 'Implications of low-pass filtering on power spectra and autocorrelation functions of turbulent velocity signals', *Mathematical Geology*, **29**, 653–668.
Soulsby, R. L. 1980. 'Selecting record length and digitisation rate for near-bed measurements', *Journal of Physical Oceanography*, **10**, 208–219.
Thomson, R. E., Gordon, R. L. and Dymond, J. 1989. 'Acoustic Doppler profiler observations of a mid-ocean hydrothermal plume', *Journal of Geophysical Research*, **94**, 4709–4720.
Voulgaris, G. and Trowbridge, J. H. 1998. 'Evaluation of the acoustic Doppler velocimeter for turbulence measurements', *Journal of Atmospheric and Oceanic Technology*, **15**, 272–289.
Zedel, L., Hay, A. E., Cabrera, R. and Lohrmann, A. 1996. 'Performance of a single-beam pulse-to-pulse coherent Doppler profiler', *IEEE Journal of Coastal Engineering*, **21**, 290–297.

